[2] S. Gottschalk, M. C. Lin, and T. Manocha, "OBBTree: A hierarchical structure for rapid interference detection," in *Proc. ACM SIGGRAPH*, 1995, pp. 171–180.
[3] S. Redon, A. Kheddar, and S. Coquillart, "Fast continuous collision detection between rigid bodies," *Comput. Graph. Forum*, vol. 21, no. 3, pp. 279–288, 2002.
[4] P. M. Hubbard, "Approximating polyhedral with spheres for time-critical collision detection," *ACM Trans. Graph.*, vol. 15, no. 3, pp. 179–210, 1996.
[5] S. Quilan, "Efficient distance computation between non-convex objects," in *Proc. IEEE Int. Conf. Robot. Autom.*, 1994, pp. 3324–3329.
[6] E. J. Bernabeu, J. Tornero, and M. Tomizuka, "Collision prediction and avoidance amidst moving objects for trajectory planning applications," in *Proc. IEEE Int. Conf. Robot. Autom.*, 2001, pp. 3801–3806.
[7] S. Cameron, "Collision detection by four-dimensional intersection testing," *IEEE Trans. Robot. Autom.*, vol. 6, no. 3, pp. 291–302, Jun. 1990.
[8] D. S. Coming and O. G. Staadt, "Velocity-aligned discrete oriented polytopes for dynamic collision detection," *IEEE Trans. Vis. Comput. Graph.*, vol. 14, no. 1, pp. 1–12, Jan./Feb. 2008.
[9] E. G. Gilbert, D. W. Johnson, and S. S. Keerthi, "A fast procedure for computing the distance between complex objects in 3D space," *IEEE J. Robot. Autom.*, vol. 4, no. 2, pp. 193–203, Apr. 1988.
[10] G. v. d. Bergen, "A fast and robust GJK implementation for collision detection of convex objects," *J. Graph. Tools*, vol. 4, no. 2, pp. 7–25, 1999.
[11] J. Canny, "Collision detection for moving polyhedra," *IEEE Trans. Pattern Anal. Mach. Intell.*, vol. 8, no. 2, pp. 200–209, Mar. 1986.
[12] F. Schwarzer, M. Saha, and J.-C. Latombe, "Adaptive dynamic collision checking for single and multiple articulated robots in complex environments," *IEEE Trans. Robot.*, vol. 21, no. 3, pp. 338–353, Jun. 2005.
[13] D. Albocher, U. Sarel, Y.-K. Choi, G. Elber, and W. Wang, "Efficient continuous collision detection for bounding boxes under rational motion," in *Proc. IEEE Int. Conf. Robot. Autom.*, 2006, pp. 3017–3022.
[14] P. Jimenez, F. Thomas, and C. Torras, "3D collision detection: A survey," *Comput. Graph.*, vol. 25, pp. 269–285, 2001.
[15] M. C. Lin and D. Manocha, "Collision and proximity queries," in *Handbook of Discrete and Computational Geometry*, 2nd ed. New York/Boca Raton, FL: Chapman & Hall/CRC, 2004, pp. 787–808.
[16] S. M. LaValle, *Planning Algorithms*. New York: Cambridge Univ. Press, 2006.
[17] G. J. Hamlin, R. B. Kelley, and J. Tornero, "Efficient distance calculation using spherically-extended polytope (s-Tope) model," in *Proc. Int. Conf. Robot. Autom.*, 1992, vol. 3, pp. 2502–2507.
[18] E. J. Bernabeu and J. Tornero, "Hough transform for distance computation and collision avoidance," *IEEE Trans. Robot. Autom.*, vol. 18, no. 3, pp. 393–398, Jun. 2002.
[19] D. Ferguson, M. Darms, C. Ursom, and S. Kolski, "Detection, prediction, and avoidance of dynamic obstacles," in *Proc. IEEE Intell. Veh. Symp.*, 2008, pp. 1149–1154.
[20] C. Urmson, J. Anhalt, D. Bagnell, C. Baker, R. Bittner, M. N. Clark, J. Dolan, D. Duggins, T. Galatali, C. Geyer, M. Gittleman, S. Harbaugh, M. Hebert, T. M. Howard, S. Kolski, A. Kelly, M. Likhachev, M. McNaughton, N. Miller, K. Peterson, B. Pilnick, R. Rajkumar, P. Rybski, B. Salesky, Y.-W. Seo, S. Singh, J. Snider, A. Stentz, W. Whittaker, Z. Wolkowicki, J. Ziglar, H. Bae, T. Brown, D. Demitrish, B. Litkouhi, J. Nickolaou, V. Sadekar, W. Zhang, M. Darms, and D. Ferguson, "Autonomous driving in urban environments: Boss and the urban challenge," *J. Field Robot.*, vol. 25, no. 8, pp. 425–466, 2008.

Swing-Up Control of the Pendubot: An Impulse–Momentum Approach

Thamer Albahkali, Ranjan Mukherjee, and Tuhin Das

***Abstract*—The standard control problem of the pendubot refers to the task of stabilizing its equilibrium configuration with the highest potential energy. Linearization of the dynamics of the pendubot about this equilibrium results in a completely controllable system and allows a linear controller to be designed for local asymptotic stability. For the underactuated pendubot, the important task is, therefore, to design a controller that will swing up both links and bring the configuration variables of the system within the region of attraction of the desired equilibrium. This paper provides a new method for swing-up control based on a series of rest-to-rest maneuvers of the first link about its vertically upright configuration. The rest-to-rest maneuvers are designed such that each maneuver results in a net gain in energy of the second link. This results in swing-up of the second link and the pendubot configuration reaching the region of attraction of the desired equilibrium. A four-step algorithm is provided for swing-up control followed by stabilization. Simulation results are presented to demonstrate the efficacy of the approach.**

***Index Terms*—Impulse, momentum, pendubot, underactuated.**

NOMENCLATURE

For the following nomenclature, $i \in \{1, 2\}$, and $j \in \{1, 6\}$.

C_i	$\cos\theta_i$.
C_{12}	$\cos(\theta_1 + \theta_2)$.
d_i	Distance between the ith joint and center of mass of the ith link (in meters).
E_2	Total energy of the second link (in Joules).
E_{2T}	Potential energy of the second link when $(\theta_1, \theta_2) = (\pi/2, 0)$ (in Joules).
F	Force acting on the second link at the second joint along the direction of motion of the second joint, which does positive work on the second link (in Newtons).
F_{imp}	Impulsive force acting on the second link at the second joint (in Newtons).
F_x	Force acting on the second link at the second joint along the x-direction (in Newtons).
F_y	Force acting on the second link at the second joint along the y-direction (in Newtons).
g	Acceleration due to gravity (9.81 $\mathrm{m/s^2}$).
I_i	Mass moment of inertia of the ith link about its center of mass (in kilograms · square meter)
l_i	Length of the ith link (in meters).
m_i	Mass of the ith link (in kilograms).
M_{imp}	Impulsive moment acting on the second link at its center of mass (in Newtons · meter).
q_j	Constants whose values depend on kinematic and dynamics parameters of the pendubot.

Manuscript received September 30, 2008; revised February 11, 2009 and April 17, 2009. First published June 5, 2009; current version published July 31, 2009. This paper was recommended for publication by Associate Editor W. Chung and Editor W. K. Chung upon evaluation of the reviewers' comments. This paper was presented at the 2008 IEEE/Robotics Society of Japan International Conference on Intelligent Robots and Systems, Nice, France.

T. Albahkali and R. Mukherjee are with the Department of Mechanical Engineering, Michigan State University, East Lansing, MI 48824 USA (e-mail: albahkal@msu.edu; mukherji@egr.msu.edu).

T. Das is with the Department of Mechanical Engineering, Rochester Institute of Technology, Rochester, NY 14623 USA (e-mail: tkdeme@rit.edu).

Digital Object Identifier 10.1109/TRO.2009.2022427

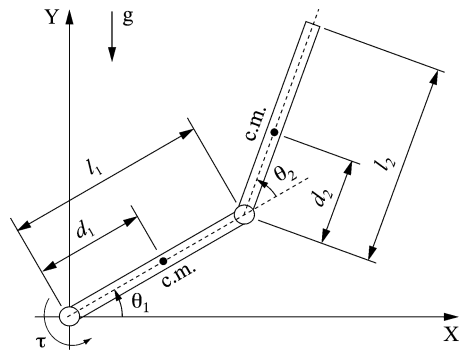

Fig. 1. Pendubot in an arbitrary configuration. The joint angles θ_1 and θ_2 are measured counterclockwise with respect to the horizontal axis.

R_A Region of attraction of the desired equilibrium $(\theta_1, \dot{\theta}_1, \theta_2, \dot{\theta}_2) = (\pi/2, 0, 0, 0)$.
S_i $\sin\theta_i$.
S_{12} $\sin(\theta_1 + \theta_2)$.
v_2 Velocity of the center of mass of the second link (in meters per second).
v_2^- Velocity of the center of mass of the second link, immediately before the first link is stopped (in meters per second).
v_2^+ Velocity of the center of mass of the second link, immediately after the first link is stopped (in meters per second).
xy Cartesian reference frame fixed to the second link.
XY Inertial reference frame with unit vectors $\vec{i}$ and $\vec{j}$ along the X- and Y-axis, respectively.
θ_i Angular displacement of the ith link, as defined in Fig. 1 (in radians).
$\dot{\theta}_i$ Angular velocity of the ith link (in radians per second).
$\dot{\theta}_i^-$ Angular velocity of the ith link, immediately before the first link is stopped (in radians per second).
$\dot{\theta}_2^+$ Angular velocity of the second link, immediately after the first link is stopped (in radians per second).
τ External torque applied on the first link (in Newtons · meter).
τ_b External torque required for braking, i.e., causing exponential decay in the velocity of the first link (in Newtons · meter).
τ_c Control torque applied during rest-to-rest maneuver prior to braking (in Newtons · meter).
τ_h External torque required to hold the first joint fixed, i.e., set $\dot{\theta}_1 = 0$ (in Newtons · meter).

I. Introduction

The pendubot [4], [21] is a two-link robot in the vertical plane with an actuator at the shoulder joint and a passive elbow joint. It is a classical example of an underactuated system [3], [16], [22], and its control problem has similarities with that of the acrobot and the single and double inverted pendulums on a cart. The complete control of the pendubot requires swing-up to the neighborhood of its equilibrium configuration with the highest potential energy followed by stabilization.

The stabilization problem, also known as the balancing problem, has been addressed by several researchers. For example, Spong and Block [21] linearized the dynamic equations and used a linear quadratic regulator, Erdem and Alleyne [6] demonstrated a large region of attraction using nonlinear control based on state-dependent Riccati equation, and Zhang and Tarn [29] used hybrid control. We linearize the dynamic equations and use a linear controller for stabilization, but the contribution of this paper lies in the development of a new methodology for swing-up of the pendubot.

Several methods have been proposed in the literature for swing-up of the pendubot. Spong and Block [21] proposed a method based on feedback linearization, and Fantoni *et al.* [7] utilized passivity properties of the pendubot to develop an energy-based controller. The controller of Fantoni *et al.* [7] requires tuning of parameters for an acceptable rate of convergence and imposes restrictions on the initial conditions to avoid a singularity. Kolesnichenko and Shiriaev [12] proposed global feedback transformations for passivity-based control, and Lai *et al.* [13] used a Lyapunov function with a time-varying parameter to avoid the singularity problem. A different approach to the problem, based on limit cycle oscillations in zero dynamics of the pendubot, was adopted by Grognard and Canudas-de-Wit [11] and Orlov *et al.* [17]. In contrast to the energy-based method [7], where the pendubot moves in a homoclinic orbit, these methods achieve orbital stabilization. Orlov *et al.* [17] and Qian *et al.* [25] used sliding-mode control to deal with uncertainties and external disturbances. A sliding-mode controller typically provides ultimate boundedness, and this motivated the zeno-mode control design by Orlov *et al.* [18]. Zeno-mode controllers require infinite switchings, and hardware implementation [19] results in chattering. The theoretical and experimental results of Freidovich *et al.* [9] are similar to the work of Grognard and Canudas-de-Wit [11] and impose virtual holonomic constraints to generate periodic motions of the passive link. Other approaches to swing-up of the pendubot include fuzzy control [14], for example.

All swing-up methods essentially aim to increase the energy of the pendubot. Our method is no exception, but we focus on the force of interaction between the two links and the work done by this force on the second link. For swing-up of the pendubot, we instinctively take the first link to the vertically upright position and conduct a series of rest-to-rest maneuvers about this configuration that results in swing-up of the second link. Similar to the work of Fantoni *et al.* [7], our approach is based on the energy of the system, but it does not impose restrictions on the initial conditions or suffer from any singularity. Furthermore, the rest-to-rest maneuvers allow swing-up in the presence of joint limit restrictions on the first link. A salient feature of our approach is the use of impulsive torques for the rest-to-rest maneuvers. The idea of using impulsive forces as control inputs is not new, and some of the early work can be credited to Pavlidis [20], Gilbert and Harasty [10], and Menaldi [15]. In recent years, researchers have investigated the problems of stability, controllability, observability, optimality, etc. (see [5], [23], [28], and the references therein), but interestingly, there has been some work on impulse control of underactuated systems. For example, Weibel *et al.* [27] investigated impulse control of a pendulum on a cart, and Aoustin *et al.* [2] investigated control of a biped robot. Wang *et al.* [26] addressed swing-up control of the Furuta pendulum, but a step pulse in the control action, which is a deviation from the standard terminology, is referred to as impulse control. The use of impulsive force provides the scope for a large change in velocity over a short time interval, and this property is exploited in this paper for swing-up of the second link with joint limit restrictions imposed on the first link. Our impulse–momentum approach can be profitably applied to control problems of other underactuated systems, such as the acrobot and biped robots, but we do not discuss these problems here to focus on the pendubot problem.

This paper is organized as follows. In Section II, we present the dynamics of the pendubot and derive expressions for the force of interaction between the two links, the holding torque, and the braking torque. In Section III, we design rest-to-rest maneuvers of the first link about its vertically upright configuration that results in net gain in energy of the second link. It is assumed that the first link is quickly brought to rest at the end of each maneuver by the application of an impulsive braking torque. The algorithm for swing-up and subsequent stabilization of

the desired equilibrium is presented in Section IV. Section V provides simulation results based on pendubot parameters in the literature. In this section, we additionally validate the impulse–momentum model of rapid braking and compare the control effort required by our algorithm with that in the literature. Section VI provides concluding remarks.

II. System Dynamics

A. Equations of Motion

Consider the pendubot in Fig. 1. Assuming no friction in the joints, the equation of motion can be obtained using the Lagrangian formulation as follows [8]:

$$A(\theta)\ddot{\theta} + B(\theta,\dot{\theta})\dot{\theta} + G(\theta) = T \tag{1}$$

where

$$\theta = \begin{pmatrix} \theta_1 \\ \theta_2 \end{pmatrix} \qquad T = \begin{pmatrix} \tau \\ 0 \end{pmatrix} \tag{2}$$

and $A(\theta)$, $B(\theta,\dot{\theta})$, and $G(\theta)$ given by the expressions

$$A(\theta) = \begin{bmatrix} q_1 + q_2 + 2q_3C_2 & q_2 + q_3C_2 \\ q_2 + q_3C_2 & q_2 \end{bmatrix} \tag{3}$$

$$B(\theta,\dot{\theta}) = q_3S_2 \begin{bmatrix} -\dot{\theta}_2 & -(\dot{\theta}_1 + \dot{\theta}_2) \\ \dot{\theta}_1 & 0 \end{bmatrix} \tag{4}$$

$$G(\theta) = g \begin{bmatrix} q_4C_1 + q_5C_{12} \\ q_5C_{12} \end{bmatrix} \tag{5}$$

are the inertia matrix, matrix containing terms resulting in the Coriolis and centrifugal forces, and vector of gravity forces, respectively. In (3)–(5), q_i, $i = 1, 2, \ldots, 5$ are constants and have the following expressions:

$$\begin{aligned} q_1 &= m_1d_1^2 + m_2l_1^2 + I_1 \\ q_2 &= m_2d_2^2 + I_2 \\ q_3 &= m_2l_1d_2 \\ q_4 &= m_1d_1 + m_2l_1 \\ q_5 &= m_2d_2. \end{aligned} \tag{6}$$

The previous constants q_j's are the same as the constants θ_j's, $j = 1, 2, \ldots, 5$ in the literature [7], [19], for example.

B. Force of Interaction Between the Two Links

By applying the Newton–Euler method [8], the forces of interaction between the two links can be computed as follows:

$$\begin{aligned} F_x &= m_2\left[-d_2(\dot{\theta}_1 + \dot{\theta}_2)^2 + l_1(\ddot{\theta}_1S_2 - \dot{\theta}_1^2C_2) + gS_{12}\right] \\ F_y &= m_2\left[d_2(\ddot{\theta}_1 + \ddot{\theta}_2) + l_1(\ddot{\theta}_1C_2 + \dot{\theta}_1^2S_2) + gC_{12}\right]. \end{aligned} \tag{7}$$

The forces F_x and F_y act along the x- and y-direction, respectively, as shown in Fig. 2. The resultant of F_x and F_y, denoted as F_R, can be decomposed into a workless constraint force along the length of the first link and the component F that does positive work on the second link. The component F can be expressed in terms of F_x and F_y as follows:

$$\begin{aligned} F &= F_x\,S_2 + F_y\,C_2 \\ &= m_2\left[l_1\ddot{\theta}_1 + d_2(\ddot{\theta}_1 + \ddot{\theta}_2)C_2 - d_2(\dot{\theta}_1 + \dot{\theta}_2)^2S_2 + gC_1\right]. \end{aligned} \tag{8}$$

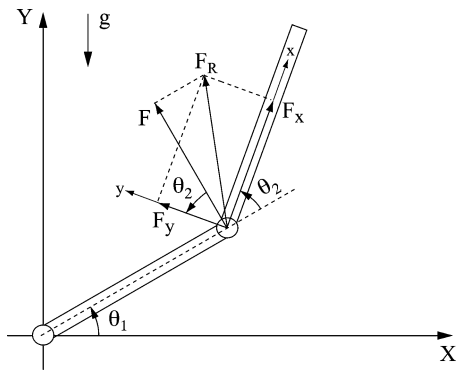

Fig. 2. Forces of interaction between the two links of the pendubot.

The total energy of the second link can be expressed as follows:

$$E_2 = \frac{1}{2}I_2(\dot{\theta}_1 + \dot{\theta}_2)^2 + \frac{1}{2}m_2\vec{v}_2 \cdot \vec{v}_2 + m_2\,g(l_1S_1 + d_2S_{12}) \tag{9}$$

where $\vec{v}_2$ is given by the expression

$$\begin{aligned} \vec{v}_2 = &-\left[l_1\,\dot{\theta}_1S_1 + d_2(\dot{\theta}_1 + \dot{\theta}_2)S_{12}\right]\vec{i} \\ &+ \left[l_1\,\dot{\theta}_1C_1 + d_2(\dot{\theta}_1 + \dot{\theta}_2)C_{12}\right]\vec{j}. \end{aligned} \tag{10}$$

By differentiating the expression for E_2, we get

$$\begin{aligned} \dot{E}_2 = &\; m_2l_1\dot{\theta}_1 \\ &\times \left[l_1\ddot{\theta}_1 + d_2(\ddot{\theta}_1 + \ddot{\theta}_2)C_2 - d_2(\dot{\theta}_1 + \dot{\theta}_2)^2S_2 + gC_1\right]. \end{aligned} \tag{11}$$

Using (8), we can verify that $\dot{E}_2 = F\,l_1\dot{\theta}_1$. This is not surprising since $l_1\dot{\theta}_1$ is the velocity of the point of application of the force F and has the same direction as that of F.

C. Holding Torque

We compute the torque required to hold the first link fixed, i.e., set $\dot{\theta}_1 = 0$. By substituting $\dot{\theta}_1 = \ddot{\theta}_1 = 0$ in (1), we get

$$\begin{bmatrix} q_2 + q_3C_2 \\ q_2 \end{bmatrix}\ddot{\theta}_2 - \begin{bmatrix} q_3S_2\,\dot{\theta}_2^2 \\ 0 \end{bmatrix} + g\begin{bmatrix} q_4C_1 + q_5C_{12} \\ q_5C_{12} \end{bmatrix} = \begin{pmatrix} \tau_h \\ 0 \end{pmatrix}. \tag{12}$$

By eliminating $\ddot{\theta}_2$ from the equations in (12), τ_h can be expressed as follows:

$$\tau_h = -q_3S_2\,\dot{\theta}_2^2 + g\left[q_4C_1 - \frac{q_3q_5}{q_2}C_2C_{12}\right]. \tag{13}$$

The holding torque in (13) will be used in Section IV in our algorithm for swing-up control.

D. Braking Torque

We consider braking action that results in exponential decay of $\dot{\theta}_1$ to zero. Therefore, we assume

$$\ddot{\theta}_1 = -k_1\dot{\theta}_1, \qquad k_1 > 0 \tag{14}$$

where k_1 is a positive constant that will control the rate of decay of $\dot{\theta}_1$. To compute the torque required for braking, we multiply (1) with the inverse of the inertia matrix to obtain

$$\begin{pmatrix} \ddot{\theta}_1 \\ \ddot{\theta}_2 \end{pmatrix} = \frac{1}{q_1q_2 - q_3^2C_2^2}\begin{bmatrix} q_2\tau + h_1 \\ -(q_2 + q_3C_2)\tau + h_2 \end{bmatrix} \tag{15}$$

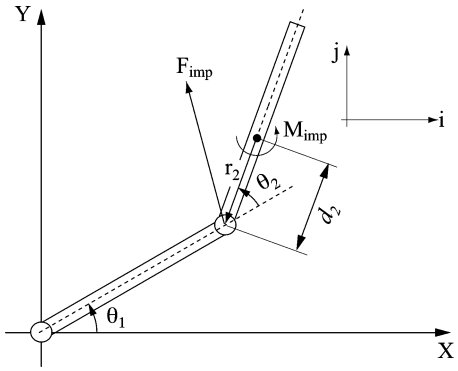

Fig. 3. Effect of suddenly stopping the first link of the pendubot.

where h_1 and h_2 are given by the expressions

$$h_1 = q_2 q_3 (\dot{\theta}_1 + \dot{\theta}_2)^2 S_2 + q_3^2 \dot{\theta}_1^2 S_2 C_2 + g(q_3 q_5 C_2 C_{12} - q_2 q_4 C_1) \tag{16}$$

$$\begin{aligned} h_2 = &-(\dot{\theta}_1 + \dot{\theta}_2)^2 (q_2 q_3 + q_3^2 C_2) S_2 \\ &- (q_1 + q_3 C_2) q_3 \dot{\theta}_1^2 S_2 - g \{ q_3 q_5 C_2 C_{12} \\ &- (q_2 + q_3 C_2) q_4 C_1 + q_1 q_5 C_{12} \}. \end{aligned} \tag{17}$$

By substituting (14) in the first equation of (15), we get

$$\tau_b = -\frac{1}{q_2} \left[k_1 \dot{\theta}_1 (q_1 q_2 - q_3^2 C_2^2) + h_1 \right]. \tag{18}$$

When the first joint comes to rest, the braking torque becomes equal to the holding torque. This can be verified from (13) and (18).

III. Energy Considerations of the Second Link

A. Effect of Suddenly Stopping the First Link

A large value of gain k_1 in the expression for the braking torque in (18) will result in sudden stopping of the first link. This action of suddenly stopping the first link has the effect of an impulsive force and an impulsive moment being applied on the second link, as shown in Fig. 3. The impulsive force results in a change in linear momentum of the second link, and the impulsive moment results in a change in angular momentum. The change in momenta can be expressed as follows:

$$\vec{F}_{\text{imp}} \, \Delta t = m_2 \, (\vec{v_2^+} - \vec{v_2^-}) \tag{19}$$

$$\vec{M}_{\text{imp}} \, \Delta t = \vec{r_2} \times \vec{F}_{\text{imp}} \, \Delta t = I_2 \, \dot{\theta}_2^+ - I_2 \, (\dot{\theta}_1^- + \dot{\theta}_2^-) \tag{20}$$

where Δt is the short interval of time over which the impulsive force and impulsive moment act, and $\vec{v_2^+}$ and $\vec{v_2^-}$ are given by the expressions

$$\vec{v_2^+} = d_2 \, \dot{\theta}_2^+ \, (-S_{12} \vec{i} + C_{12} \vec{j}) \tag{21}$$

$$\begin{aligned} \vec{v_2^-} = &- \left[l_1 \, \dot{\theta}_1^- S_1 + d_2 (\dot{\theta}_1^- + \dot{\theta}_2^-) S_{12} \right] \vec{i} \\ &+ \left[l_1 \, \dot{\theta}_1^- C_1 + d_2 (\dot{\theta}_1^- + \dot{\theta}_2^-) C_{12} \right] \vec{j} \end{aligned} \tag{22}$$

which can be obtained from (10). The vector $\vec{r_2}$ is shown in Fig. 3 and has the form

$$\vec{r_2} = -d_2 (C_{12} \vec{i} + S_{12} \vec{j}). \tag{23}$$

Substituting (19), (21), (22), and (23) into (20), we get

$$\dot{\theta}_2^+ = \dot{\theta}_2^- + \left[1 + \frac{l_1 m_2 d_2 C_2}{I_2 + m_2 d_2^2} \right] \dot{\theta}_1^-. \tag{24}$$

Since there is no change in potential energy over the time interval Δt, the change in total energy of the second link is due to the change in its kinetic energy alone and is equal to

$$\begin{aligned} \Delta E_2 = &\frac{1}{2} (I_2 + m_2 d_2^2) (\dot{\theta}_2^+)^2 - \frac{1}{2} I_2 \left(\dot{\theta}_1^- + \dot{\theta}_2^- \right)^2 \\ &- \frac{1}{2} m_2 \left[l_1^2 \, (\dot{\theta}_1^-)^2 + d_2^2 (\dot{\theta}_1^- + \dot{\theta}_2^-)^2 \, + 2 l_1 d_2 \dot{\theta}_1^- (\dot{\theta}_1^- + \dot{\theta}_2^-) C_2 \right]. \end{aligned} \tag{25}$$

By substituting (24) into (25), we express the change in the total energy of the second link in terms of the velocity of the first link prior to stopping as follows:

$$\Delta E_2 = \frac{1}{2} m_2 l_1^2 \left[\frac{m_2 d_2^2 C_2^2}{I_2 + m_2 d_2^2} - 1 \right] (\dot{\theta}_1^-)^2. \tag{26}$$

Since $m_2 d_2^2 C_2^2 < (I_2 + m_2 d_2^2)$, $\Delta E_2 \leq 0$ and $\Delta E_2 = 0$, if and only if $\dot{\theta}_1^- = 0$. Clearly, the total energy of the second link decreases whenever the first link is stopped suddenly.

B. Rest-to-Rest Maneuver of the First Link

Consider a maneuver in which the first joint starts from rest and is brought back to rest through the application of a braking torque using a large gain k_1. Taking into account the loss of energy due to sudden stopping, which is given by (26), the net work done on the second link due to the rest-to-rest maneuver can be computed as follows:

$$\begin{aligned} \Delta E_2 &= \int F \, l_1 \, d\theta_1 + \frac{1}{2} m_2 l_1^2 \left[\frac{m_2 d_2^2 C_2^2}{I_2 + m_2 d_2^2} - 1 \right] (\dot{\theta}_1^-)^2 \\ &\geq \int F \, l_1 \, \dot{\theta}_1 \, dt - \frac{1}{2} m_2 l_1^2 (\dot{\theta}_1^-)^2 \end{aligned} \tag{27}$$

where F is given by the expression in (8). To ensure $\Delta E_2 > 0$, we choose F as follows:

$$F = m_2 \left[(1 + k_2) l_1 \, \ddot{\theta}_1 \right] \tag{28}$$

where k_2 is a positive constant. Indeed, substitution of (28) into (27) gives

$$\begin{aligned} \Delta E_2 &\geq l_1 \int F \, \dot{\theta}_1 \, dt - \frac{1}{2} m_2 l_1^2 (\dot{\theta}_1^-)^2 \\ &= l_1 \int m_2 \left[(1 + k_2) l_1 \, \ddot{\theta}_1 \right] \dot{\theta}_1 \, dt - \frac{1}{2} m_2 l_1^2 (\dot{\theta}_1^-)^2 \\ &= \left[\frac{1 + k_2}{2} \right] m_2 \, l_1^2 \int 2 \dot{\theta}_1 \ddot{\theta}_1 \, dt - \frac{1}{2} m_2 l_1^2 (\dot{\theta}_1^-)^2 \\ &= \left[\frac{1 + k_2}{2} \right] m_2 \, l_1^2 (\dot{\theta}_1^-)^2 - \frac{1}{2} m_2 l_1^2 (\dot{\theta}_1^-)^2 \\ &= \frac{1}{2} k_2 \, m_2 \, l_1^2 (\dot{\theta}_1^-)^2 > 0. \end{aligned} \tag{29}$$

By equating (8) and (28), we get the constraint

$$d_2 (\ddot{\theta}_1 + \ddot{\theta}_2) C_2 - d_2 (\dot{\theta}_1 + \dot{\theta}_2)^2 S_2 + g C_1 = k_2 \, l_1 \ddot{\theta}_1.$$

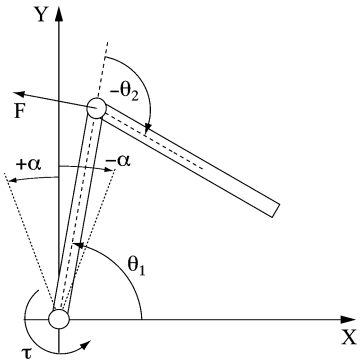

Fig. 4. For the rest-to-rest maneuvers, the first link configuration satisfies $(\pi/2-\alpha) \le \theta_1 \le (\pi/2+\alpha)$.

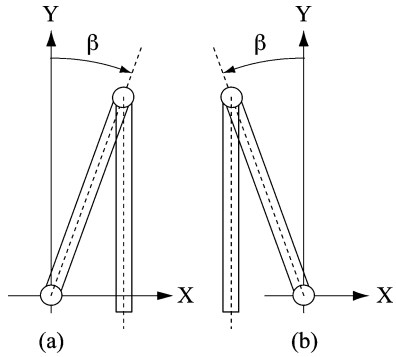

Fig. 5. Second link is shown in its "vertically down" configuration during a rest-to-rest maneuver.

Substitution of this constraint in (1) gives us the expression for the control torque

$$\tau_c = \left[\frac{q_1 q_2 - q_3^2 C_2^2}{k_2 l_1 q_2 + d_2 q_3 C_2^2}\right] \left\{gC_1 - d_2(\dot\theta_1+\dot\theta_2)^2 S_2\right\} + \left[\frac{1}{k_2 l_1 q_2 + d_2 q_3 C_2^2}\right] \{d_2(h_1+h_2)C_2 - k_2 l_1 h_1\} \quad (30)$$

where h_1 and h_2 were defined earlier by (16) and (17), respectively. From the analysis in this section, it is clear that the net value of E_2 will increase if the first joint is driven using the torque expression in (30) and then stopped suddenly.

It is important to note that at any time during a rest-to-rest maneuver, while the first link is still in motion, it is possible to compute

1) E_2 from the values of θ_1, $\dot\theta_1$, θ_2, and $\dot\theta_2$;
2) energy loss that would result from stopping the first link instantaneously from (26).

When the difference of the energy values in 1) and 2) is equal to E_{2T}, the motion of the first link can be quickly stopped so that $E_2 \approx E_{2T}$.

IV. Algorithm for Swing-Up Control

A four-step algorithm is proposed for swing-up control of the pendubot followed by asymptotic stabilization of the desired equilibrium. We define two constants that appear in the discussion of the algorithm

$$q_6 \equiv \sqrt{\frac{m_2 g l_1}{q_2}}, \qquad q_7 \equiv \frac{m_2 d_2^2}{q_2} < 1.$$

1) *Initialization:*
   a) Linearize the dynamic equations of the pendubot in (1) about the desired equilibrium $(\theta_1, \dot\theta_1, \theta_2, \dot\theta_2) = (\pi/2, 0, 0, 0)$.
   b) Design a linear controller to render the desired equilibrium locally asymptotically stable. Let R_A define the region of attraction of the desired equilibrium.
   c) Choose a small angle α, $\alpha > 0$ such that the configuration $(\theta_1, \dot\theta_1, \theta_2, \dot\theta_2) = [\pi/2 - \gamma, 0, \gamma, 2q_6 \sin(\gamma/2)]$ lies inside R_A for all values of $\gamma \in [-\alpha, \alpha]$. This will always be possible since this configuration converges to the desired equilibrium $(\pi/2, 0, 0, 0)$ as $\alpha \to 0$.
2) *Swing-up control of the first link:*
   Drive the first link from its initial configuration to any configuration that satisfies $(\pi/2-\alpha) \le \theta_1 \le (\pi/2+\alpha)$, $\dot\theta_1 = 0$, as shown in Fig. 4.
3) *Swing-up control of the second link:*
   a) Conduct rest-to-rest maneuvers of the first link about the vertically upright configuration with θ_1 satisfying $(\pi/2-\alpha) \le \theta_1 \le (\pi/2+\alpha)$. From our discussion in the last section, we know that each rest-to-rest maneuver will increase the value of E_2. In particular, the following procedure will be adopted: The holding torque, i.e., τ_h in (13), will be applied to hold the first link fixed. To initiate the motion of the first link in the positive (counterclockwise) direction, the torque expression in (30) will be used when it is greater than τ_h—see Discussion 1 after the fourth step of the algorithm. To initiate the motion of the first link in the negative (clockwise) direction, the torque expression in (30) will be used when it is less than τ_h—see Discussion 1. As the first link approaches the boundary of the interval $[(\pi/2-\alpha), (\pi/2+\alpha)]$, the braking torque τ_b in (18) will be used; a large value of k_1 will be used to quickly stop the motion of the first link.
   b) Terminate the rest-to-rest maneuvers with $E_2 \approx E_{2T}$. From our discussion in the last section, we know that this can be accomplished by monitoring the states of the pendubot. Then, the pendubot configuration will satisfy $(\pi/2-\alpha) \le \theta_1 \le (\pi/2+\alpha)$, $\dot\theta_1 = 0$, and $E_2 \approx E_{2T}$.
4) *Stabilization:*
   With $(\pi/2-\alpha) \le \theta_1 \le (\pi/2+\alpha)$, $\dot\theta_1 = 0$, and $E_2 \approx E_{2T}$, the second link will behave like a pendulum. When the second link reaches its highest potential energy configuration, the pendubot configuration will be inside R_A—see Discussion 2. Invoke the linear controller, which is designed in the first step of the algorithm, to stabilize the desired equilibrium.

Discussion 1

For swing-up of the second link in the third step of the algorithm, τ_c has to be greater than τ_h for some values of θ_2, $\dot\theta_2$ and less than τ_h for other values of θ_2, $\dot\theta_2$ when $(\pi/2-\alpha) \le \theta_1 \le (\pi/2+\alpha)$ and $\dot\theta_1 = 0$. We now show that these conditions will indeed be satisfied. For $\dot\theta_1 = 0$, the difference in the torques can be shown to be equal to

$$\Pi(\theta_1, \theta_2, \dot\theta_2) \equiv (\tau_c - \tau_h)_{\dot\theta_1 = 0} = g\,[C_1 - q_7\, C_2 C_{12}] - d_2 S_2 \dot\theta_2^2. \quad (31)$$

Now consider the joint configuration $(\theta_1, \theta_2) = (\pi/2 - \beta, -\pi + \beta)$, $\beta \in (0, \alpha]$, as shown in Fig. 5(a), where the second link is vertically down. During swing-up, the second link has to pass through this configuration. Since $S_2 = -\sin\beta < 0$, we have the following

TABLE 1
COMPARISON OF SIMULATION RESULTS OF BRAKING WITH ANALYTICAL RESULTS OF SUDDEN STOPPING

k_1	$\Delta t\ (sec)$	$\Delta\theta_1\ (rad)$	$\dot{\theta}_2^+\ (rad/s)$	difference (%)	$\Delta E_2\ (J)$	difference (%)
100	0.060	0.020	5.416	20.15	-0.0021	43.24
1000	0.006	0.002	6.547	3.48	-0.0035	5.4
2000	0.003	0.001	6.650	1.96	-0.0036	2.7

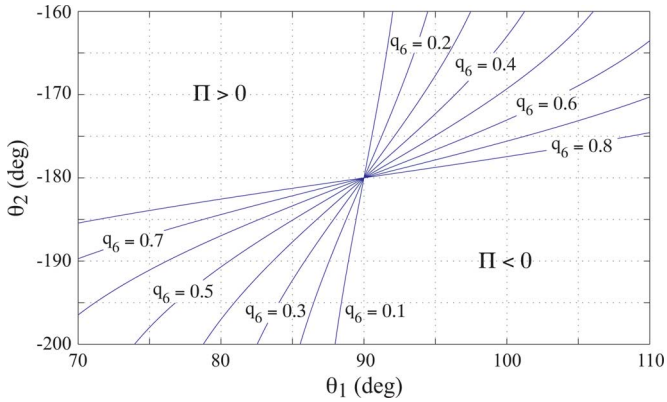

Fig. 6. Plot showing regions in the θ_1–θ_2 space, where $\Pi > 0$ and $\Pi < 0$.

from (31):

$$\Pi \geq g\left[C_1 - q_6\, C_2 C_{12}\right].$$

A plot of the right-hand side of the previous equation, as shown in Fig. 6, indicates that $\Pi > 0$ for $(\theta_1, \theta_2) = (\pi/2 - \beta, -\pi + \beta)$, $\beta \in (0, \alpha]$, for feasible values of α and q_6. This implies that the control torque τ_c can move the first link in the counterclockwise direction. A similar analysis indicates that $\Pi < 0$ for the configuration $(\theta_1, \theta_2) = (\pi/2 + \beta, -\pi - \beta)$, $\beta \in (0, \alpha]$, as shown in Fig. 5(b). This configuration is, therefore, conducive for the first link to move in the clockwise direction.

Discussion 2

With $(\pi/2 - \alpha) \leq \theta_1 \leq (\pi/2 + \alpha)$, $\dot{\theta}_1 = 0$, and $E_2 \approx E_{2T}$, the second link will behave like a pendulum. At its highest potential energy configuration, the second link configuration will satisfy $\theta_2 = \pi/2 - \theta_1$. The velocity of the second link can, therefore, be computed as follows:

$$E_2|_{\dot{\theta}_1 = 0} = E_{2T} \quad \Rightarrow \quad \dot{\theta}_2^2 = 2q_6^2(1 - S_1).$$

By expressing $\theta_1 = \pi/2 - \gamma$, $\gamma \in [-\alpha, \alpha]$, we can describe the pendubot configuration as

$$(\theta_1, \dot{\theta}_1, \theta_2, \dot{\theta}_2) = \left[\frac{\pi}{2} - \gamma, 0, \gamma, 2q_6 \sin\left(\frac{\gamma}{2}\right)\right]$$

which lies inside R_A through choice of α during initialization.

V. NUMERICAL SIMULATIONS

We present simulation results for two sets of kinematic and dynamic parameters of the pendubot. The first set of parameters, which are taken from Orlov *et al.* [17], are presented as follows:

$$\begin{aligned} m_1 &= 0.132\ \text{kg}, \quad l_1 = 0.203\ \text{m} \\ m_2 &= 0.088\ \text{kg}, \quad l_2 = 0.254\ \text{m} \\ d_1 &= 0.1574\ \text{m}, \quad I_1 = 0.00362\ \text{kg}\cdot\text{m}^2 \\ d_2 &= 0.1109\ \text{m}, \quad I_2 = 0.00114\ \text{kg}\cdot\text{m}^2. \end{aligned} \tag{32}$$

For these parameters, E_{2T} was evaluated to be 0.2710 J.

A. Impulse–Momentum Model of Braking

In Section III-A, we modeled sudden stopping of the first link by the action of an impulsive force and an impulsive moment on the second link. Here, we show that this modeling assumption is accurate for large values of gain k_1 in the expression for the braking torque in (18), which we know will cause sudden stopping of the first link. We consider the pendubot configuration $(\theta_1, \dot{\theta}_1, \theta_2, \dot{\theta}_2) = (0.0, 2.0, 0.0, 3.0)$, where the units are radians and radians per second. If the first joint is stopped instantaneously, the velocity of the second joint and change in energy of the second link can be computed using (24) and (26), respectively. Specifically, using $\dot{\theta}_1^- = 2.0$ rad/s and $\dot{\theta}_2^- = 3.0$ rad/s, these values can be computed as

$$\dot{\theta}_2^+ = 6.783\ \text{rad/s}, \qquad \Delta E_2 = -0.0037\ \text{J}. \tag{33}$$

The values of $\dot{\theta}_2^+$ and ΔE_2, which are obtained from simulations, are shown in Table I for different values of gain k_1 used in the expression for the braking torque in (18). It is clear that the difference of these values from those in (33) is negligible for large values of gain k_1. Also, as expected, large values of k_1 require less time for the first link to come to rest and small angle of travel of the first link before it comes to rest. In our simulation of swing-up control, which is presented next, we used a value of $k_1 = 1000$.

B. Swing-Up Control and Stabilization

As part of the initialization (first step of the algorithm), a linear controller is designed to stabilize the desired equilibrium. Through repeated simulation of the closed-loop system behavior, the maximum value of α is found to be $10°$.[1] The initial configuration of the pendubot is chosen as

$$(\theta_1, \dot{\theta}_1, \theta_2, \dot{\theta}_2) = (90.0, 0.0, -135.0, 0.0) \tag{34}$$

where the units are degrees and degrees per second. This choice of initial configuration eliminates the need for the second step of the algorithm, which is trivial. The simulation results for the third and fourth steps of the algorithm are shown in Fig. 7; the plots show the two joint angles, their velocities, the control torque, and the energy of the second link.

It can be seen from Fig. 7 that E_2 reaches the value of E_{2T} at $t = t_s = 2.97$ s. At this time, the second link is close to its vertically upright configuration, and the linear controller is invoked for stabilization. The swing-up control of the second link is achieved over the interval $t \in [0, 2.97]$s through a series of rest-to-rest maneuvers separated by periods of time over which the first joint is held fixed. It can be seen from Fig. 7 that E_2 increases for each rest-to-rest maneuver but remains constant during times when the first link is held fixed. The increase of E_2 during each rest-to-rest maneuver is achieved through positive work done by the first link followed by energy loss due to braking. During braking, the control torques peak, but the peak torques act over short intervals of time. This is expected since the braking torques are

[1]This value, of course, depends on the gains of the linear controller used for stabilization.

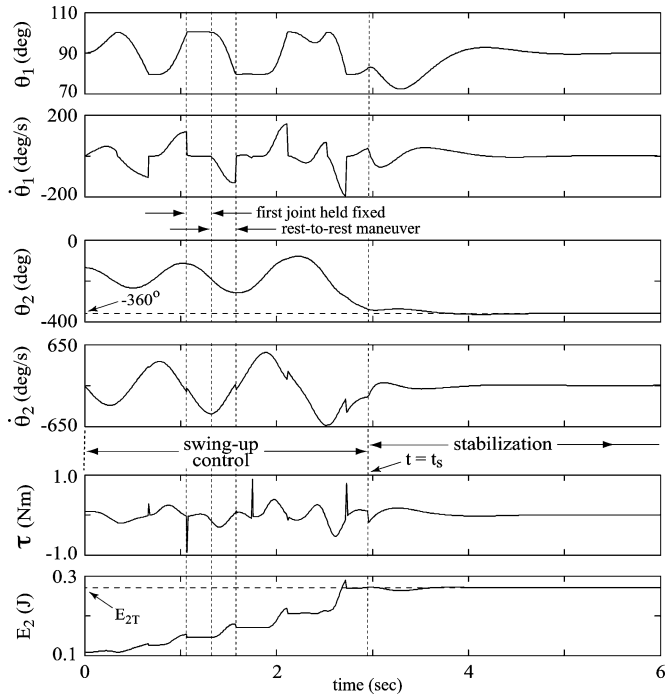

Fig. 7. Plot of joint angles, joint angle velocities, control torque, and energy of second link for the first simulation in Section V.

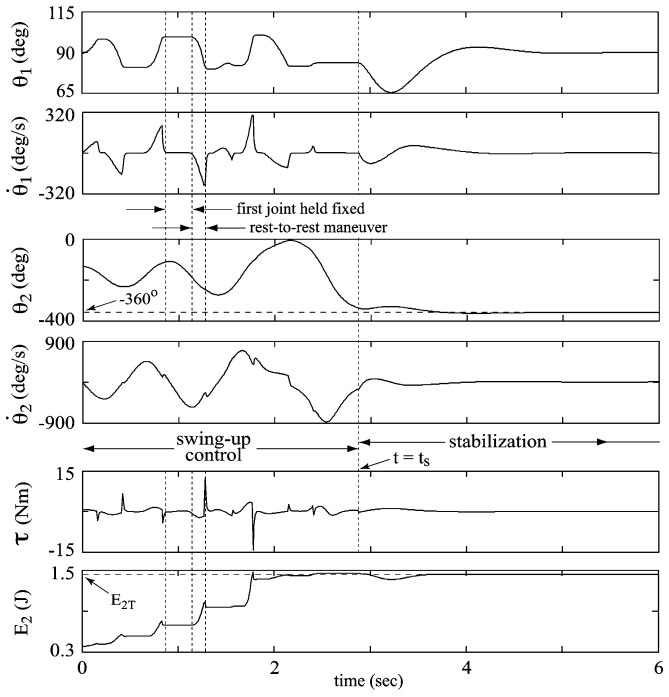

Fig. 8. Plot of joint angles, joint angle velocities, control torque, and energy of second link for the second simulation in Section V.

impulsive in nature due to the choice of a large value of gain k_1. Despite its impulsive nature, the maximum value of the torque required by our algorithm is 1.0 N·m—this is less than the maximum torque of 1.7 N·m required by the algorithm proposed by Orlov *et al.* [17].

C. Comparison With Experimental Results

It behooves us to point out that the maximum torque required by our algorithm, by virtue of being impulsive in nature, will be limited by the *peak torque* of the motor and not the *maximum continuous torque*. The peak torque of a motor is greater than the maximum continuous torque by a factor that varies from motor to motor. A search of the literature published by motor manufacturers indicates that this factor can vary in the range of 2–10 and is equal to 4 for a specific example worked out in the *Handbook of Electric Motors* [24]. To check feasibility of hardware implementation of our algorithm, we now compare our simulation results with experimental results published in the literature. To this end, we choose the following kinematic and dynamic parameters of the pendubot:

$$\begin{aligned} m_1 &= 1.0367 \text{ kg}, \qquad l_1 = 0.1508 \text{ m} \\ m_2 &= 0.5549 \text{ kg}, \qquad l_2 = 0.2667 \text{ m} \\ d_1 &= 0.1206 \text{ m}, \qquad I_1 = 0.0031 \text{ kg}\cdot\text{m}^2 \\ d_2 &= 0.1135 \text{ m}, \qquad I_2 = 0.0035 \text{ kg}\cdot\text{m}^2. \end{aligned} \tag{35}$$

The parameters result in the following values of q_j, $j \in \{1, 5\}$:

$$\begin{aligned} q_1 &= 0.0308 \text{ kg}\cdot\text{m}^2, \qquad q_2 = 0.0106 \text{ kg}\cdot\text{m}^2 \\ q_3 &= 0.0095 \text{ kg}\cdot\text{m}^2, \qquad q_4 = 0.2087 \text{ kg}\cdot\text{m}^2 \\ q_5 &= 0.0629 \text{ kg}\cdot\text{m}^2 \end{aligned} \tag{36}$$

which are almost identical to the values of θ_j ($\theta_j \equiv q_j$), $j \in \{1, 5\}$ in the paper by Orlov *et al.* [19] with experimental data for the control torque.

For the parameter values in (35), E_{2T} was computed as 1.438 J. For the initial configuration of the pendubot given by (34), the simulation results are shown in Fig. 8. It can be seen from this figure that swing-up and stabilization are achieved in less than 4 s. The maximum torque required by our algorithm is approximately 15 N·m. In the experimental work by Orlov *et al.* [19], the maximum torque required was 7 N·m for the nominal model and 30 N·m for the model with disturbances. It suffices to say that the motor used in the experimental work [19] can be used for implementation of our algorithm. A comparison of our results with the results for the nominal model alone indicates that our maximum torque is greater than the maximum torque in [19] by a factor of 2.1. This is acceptable since the torque required by our algorithm is intermittent, and its maximum value is limited by the *peak torque* of the motor, whereas the maximum torque in [19] is limited by the *maximum continuous torque* (which is much less than the peak torque [24]) due to its high-frequency components.

For our algorithm, the power requirement of the motor will be high intermittently for very brief periods of time. It is likely to exceed the power specifications of the motor, but this is not a concern since motor power specifications are based on continuous, and not intermittent, operation.

VI. Conclusion

This paper presents a new solution to the swing-up control problem of the pendubot. The solution is based on taking the first link to its vertically upright position and executing a series of rest-to-rest maneuvers about this position with a small amplitude of oscillation. Using the principles of work–energy and impulse and momentum, the rest-to-rest maneuvers are designed to increase the energy of the second link. The rest-to-rest maneuvers are carried out till the energy of the second link is approximately equal to its maximum potential energy. This results in the pendubot configuration reaching a neighborhood of the desired equilibrium from which the equilibrium can be stabilized using

a linear controller. Simulation results are presented to demonstrate the feasibility of the proposed approach. Our future work will focus on experimental verification of the swing-up control algorithm presented in this paper and extension of the impulse–momentum approach to swing-up control of the acrobot and control of other underactuated mechanical systems.

REFERENCES

[1] T. Albahkali, R. Mukherjee, and T. Das, "An impulse-momentum approach to swing-up control of the pendubot," in *Proc. IEEE/RSJ Conf. Intell. Robots Syst.*, Sep. 2008, pp. 3750–3755.

[2] Y. Aoustin, D. T. Romero, C. Chevallereau, and S. Aubin, "Impulsive control for a thirteen-link biped," in *Proc. IEEE Int. Workshop Adv. Motion Control*, Istanbul, Turkey, 2006, pp. 439–444.

[3] H. Arai and S. Tachi, "Position control of a manipulator with passive joints using dynamic coupling," *IEEE Trans. Robot. Autom.*, vol. 7, no. 4, pp. 528–534, Aug. 1991.

[4] D. J. Block, "Mechanical design and control of the pendubot," M.S. thesis, Dept. Gen. Eng., Univ. Illinois Urbana-Champaign, Urbana, 1996.

[5] J. Chudoung and C. Beck, "The minimum principle for deterministic impulsive control systems," in *Proc. IEEE Conf. Decis. Control*, Orlando, FL, 2001, pp. 3569–3574.

[6] E. B. Erdem and A. G. Alleyne, "Experimental real-time SDRE control of an underactuated robot," in *Proc. 40th IEEE Decis. Control Conf.*, Orlando, FL, 2001, pp. 2986–2991.

[7] I. Fantoni, R. Lozano, and M. W. Spong, "Energy based control of the pendubot," *IEEE Trans. Autom. Control*, vol. 45, no. 4, pp. 725–729, Apr. 2000.

[8] K. S. Fu, R. C. Gonzales, and C. S. G. Lee, *Robotics: Control, Sensing, Vision, and Intelligence*. New York: McGraw-Hill, 1987.

[9] L. Freidovich, A. Robertsson, A. Shiriaev, and R. Johansson, "Periodic motions of the pendubot via virtual holonomic constraints: Theory and experiments," *Automatica*, vol. 44, pp. 785–791, 2008.

[10] E. G. Gilbert and G. A. Harasty, "A class of fixed-time fuel-optimal impulsive control problems and an efficient algorithm for their solution," *IEEE Trans. Autom. Control*, vol. AC-16, no. 1, pp. 1–11, Feb. 1967.

[11] F. Grognard and C. Canudas-de-Wit, "Virtual constraints for the orbital stabilization of the pendubot," in *Nonlinear and Adaptive Control: Theory and Algorithms for the User*, A. Astolfi, Ed. London, U.K.: Imperial College Press, 2005, pp. 115–145.

[12] O. Kolesnichenko and A. S. Shiriaev, "Partial stabilization of underactuated Euler–Lagrange systems via a class of feedback transformations," *Syst. Control Lett.*, vol. 45, pp. 121–132, 2002.

[13] X.-Z. Lai, J.-H. She, S. X. Yang, and M. Wu, "Unified treatment of motion control of underactuated two-link manipulators," in *Proc. IEEE/RSJ Conf. Intell. Robots Syst.*, 2006, pp. 574–579.

[14] W. Li, K. Tanaka, and H. O. Wang, "Acrobatic control of a pendubot," *IEEE Trans. Fuzzy Syst.*, vol. 12, no. 4, pp. 549–552, Aug. 2004.

[15] J.-L. Menaldi, "The separation principle for impulse control problems," *Amer. Math. Soc.*, vol. 82, no. 3, pp. 439–445, 1981.

[16] R. Mukherjee and D. G. Chen, "Control of free-flying underactuated space manipulators to equilibrium manifolds," *IEEE Trans. Robot. Autom.*, vol. 9, no. 5, pp. 561–570, Oct. 1993.

[17] Y. Orlov, L. T. Aguilar, and L. Acho, "Model orbit robust stabilization (MORS) of pendubot with application to swing up control," in *Proc. 44th IEEE Int. Conf. Decis. Control*, Seville, Spain, 2005, pp. 6164–6169.

[18] Y. Orlov, L. T. Aguilar, and L. Acho, "Zeno mode control of underactuated mechanical systems with application to pendubot stabilization around the upright position," presented at the 16th IFAC World Congr., Prague, Czech Republic, 2005.

[19] Y. Orlov, L. T. Aguilar, L. Acho, and A. Ortiz, "Swing up and balancing control of pendubot via model orbit stabilization: Algorithm synthesis and experimental verification," in *Proc. IEEE Conf. Decis. Control*, 2006, pp. 6138–6143.

[20] T. Pavlidis, "Stability of systems described by differential equations containing impulses," *IEEE Trans. Autom. Control*, vol. AC-12, no. 1, pp. 43–45, Feb. 1967.

[21] M. W. Spong and D. J. Block, "The pendubot: A mechatronic system for control research and education," in *Proc. 34th IEEE Int. Conf. Decis. Control*, New Orleans, LA, 1995, pp. 555–556.

[22] M. W. Spong, "Underactuated mechanical systems," in *Control Problems in Robotics and Automation* (Lecture Notes in Control and Information Science), vol. 230, B. Siciliano and K. P. Valavanis, Eds. London, U.K.: Springer-Verlag, 1998, pp. 135–150.

[23] J. Sun, Y. Zhang, and Q. Wu, "Less conservative conditions for asymptotic stability of impulsive control systems," *IEEE Trans. Autom. Control*, vol. 48, no. 5, pp. 829–831, May 2003.

[24] H. A. Toliyat and G. B. Kliman, *Handbook of Electric Motors*, 2nd. ed. New York: Marcel Dekker, 2004, p. 354.

[25] D. Qian, J. Yi, and D. Zhao, "Hierarchical sliding mode control to swing up a pendubot," in *Proc. Amer. Control Conf.*, New York, 2007, pp. 5254–5259.

[26] Z. Wang, Y. Chen, and N. Fang, "Minimum-time swing-up of a rotary inverted pendulum by iterative impulsive control," in *Proc. Amer. Control Conf.*, 2004, pp. 1335–1340.

[27] S. Weibel, G. W. Howell, and J. Baillieul, "Control of single-degree-of-freedom Hamiltonian systems with impulsive inputs," in *Proc. IEEE Conf. Decis. Control*, Kobe, Japan, 1996, pp. 4661–4666.

[28] G. Xie and L. Wang, "Necessary and sufficient conditions for controllability and observability of switched impulsive control systems," *IEEE Trans. Autom. Control*, vol. 49, no. 6, pp. 960–966, Jun. 2004.

[29] M. Zhang and T.-J. Tarn, "Hybrid control of the pendubot," *IEEE/ASME Trans. Mechatron.*, vol. 7, no. 1, pp. 79–86, Mar. 2002.